Food Chemistry: X 25 (2025) 102179

Contents lists available at ScienceDirect

Food Chemistry: X

journal homepage: www.sciencedirect.com/journal/food-chemistry-x

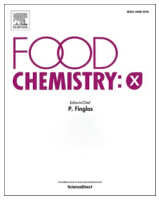

Differentiation and characterization of volatile compounds in five common milk powders using HS-GC-IMS, HS-SPME-GC–MS, and multivariate statistical approaches

Yaxi Zhou [a,b,c,1], Diandian Wang [a,b,1], Jian Zhao [b], Yu Guo [b], Wenjie Yan [a,b,*]

[a] College of Biochemical Engineering, Beijing Union University, Beijing 100023, China
[b] Beijing Key Laboratory of Bioactive Substances and Functional Food, Beijing Union University, Beijing 100023, China
[c] Institute of Apicultural Research, Chinese Academy of Agricultural Sciences, Beijing 100093, China

ARTICLE INFO

Keywords:
Milk powder
Volatile compounds
HS-GC-IMS
HS-SPME-GC–MS
OPLS-DA

ABSTRACT

Aroma is a key factor in milk powder quality evaluation and consumer choice. However, research has mostly focused on processing effects, with little on flavor differences among milk powders. This study analysed and identified the flavor characteristics of five common types of milk powders in China, including yak milk powder, donkey milk powder, camel milk powder, goat milk powder, and cow milk powder, using Headspace-Gas Chromatography-Ion Mobility Spectrometry (HS-GC-IMS), Headspace Solid-Phase Microextraction-Gas Chromatography-Mass Spectrometry (HS-SPME-GC–MS), and multivariate statistical analysis. Results identified 55 and 86 volatile compounds via HS-GC-IMS and HS-SPME-GC–MS, respectively, revealing significant differences between milk powders. PCA, OPLS-DA, PLS-DA, and heatmaps further distinguished the sources. Based on VIP values, 27 and 24 key compounds were identified. These results underscored the potential of utilizing these combined techniques for quick flavor analysis and detecting adulteration in milk powder.

1. Introduction

Currently, a wide variety of milk powders are available on the market, with most being formulated milk powders. Studies have shown that some of these formulas may exceed permissible levels of heavy metals (Sager, McCulloch, & Schoder, 2018) and may also be contaminated with mycotoxins (Yacine Ware et al., 2017). In 2020, Daniel Munblit pointed out that health and nutritional claims for infant formulas are often inadequately supported by evidence, potentially harmful to human health, and recommended that such marketing claims should be prohibited (Munblit, Crawley, Hyde, & Boyle, 2020). As a result, pure milk powders, including cow milk powder, yak milk powder, donkey milk powder, camel milk powder, and goat milk powder, are increasingly favored by consumers due to their natural, additive-free properties (Ditlevsen, Sandøe, & Lassen, 2019; Yormirzoev, Li, & Teuber, 2021).

Although consumers generally prefer pure, natural milk powders, different types of milk powders are favored by different individuals due to their distinct flavors. The flavor of milk powder, determined mainly by its taste and aroma, significantly influences consumer acceptance and choice (Pan et al., 2019). Aroma is one of the key factors in evaluating milk powder quality and impacting consumer preference. Previous research has extensively confirmed that processing methods, such as sterilization and drying techniques (Feng, Wang, Ji, Min, & Yan, 2021, 2021a), as well as storage conditions and harvest times, can affect the composition and flavor of milk powder (Zhang et al., 2024; Zhao et al., 2023). Thus, while much attention has been given to enhancing the acceptability of milk powder through processing, there has been little focus on the intrinsic flavor differences between various types of milk powder. It is evident that current research on milk powder flavor predominantly addresses the impact of processing and handling, with no studies reporting the flavor differences between different types of fresh milk powders.

In recent years, an increasing number of food analysis techniques have been applied to the study of food flavor. Common methods include headspace solid-phase microextraction gas chromatography–mass spectrometry (HS-SPME-GC–MS), gas chromatography-olfactometry-mass spectrometry (GC-O-MS), headspace-gas chromatography-ion

* Corresponding author at: College of Biochemical Engineering, Beijing Union University, Beijing 100023, China.
E-mail address: meyanwenjie@126.com (W. Yan).
[1] Yaxi Zhou and Diandian Wang contributed equally to this work.

https://doi.org/10.1016/j.fochx.2025.102179
Received 18 November 2024; Received in revised form 4 January 2025; Accepted 12 January 2025
Available online 13 January 2025

mobility spectrometry (HS-GC-IMS), and electronic nose technology (Du, Chen, Liu, Wang, & Kong, 2021; Junxing et al., 2022; Q. Zhang, Wang, Meng, Wang, & Wang, 2024). Among these, HS-GC-IMS is becoming increasingly popular for the analysis of flavor compounds due to its several distinct advantages. These include low sample volume requirements, high sensitivity, excellent detection accuracy, and ease of operation. HS-GC-IMS is especially beneficial for rapid, real-time analysis, offering high throughput and minimal sample preparation, making it ideal for the fast analysis of complex flavor profiles (Gu, Zhang, Wang, Wang, & Du, 2021; Wang, Chen, & Sun, 2020). On the other hand, HS-SPME-GC–MS is the most widely used and established method in food flavor analysis. This technique is particularly favored for its excellent sensitivity and selectivity, allowing for precise identification and quantification of volatile compounds at trace levels. HS-SPME-GC–MS is especially effective in handling complex food matrices, providing both qualitative and quantitative data on volatile compounds (Song & Liu, 2018).

In this research, HS-GC-IMS and HS-SPME-GC–MS techniques, along with multivariate statistical analyses, were applied to detect and examine volatile compounds in five widely available milk powder brands. A total of 27 and 24 key volatile compounds were identified by HS-GC-IMS and HS-SPME-GC–MS, respectively, establishing essential markers for differentiating various milk powder types. This study provides a significant reference for understanding the volatile compound profiles within milk powders, thus laying the groundwork for accurate classification and product differentiation based on these distinctive volatiles.

2. Materials and methods

2.1. Collection and processing of five milk powder samples

Our goal is to explore the differences in volatile components among different milk powder samples. Since milk powders on the market undergo different processing methods, which can directly impact our experimental results, we chose to obtain fresh samples directly from their origin and performed uniform pretreatment to reduce potential errors(Feng et al., 2021). Fresh yak milk was sourced from Hongyuan Yak Dairy Co., Ltd. (Aba Tibetan and Qiang Autonomous Prefecture, Sichuan, China); fresh donkey milk was obtained from Quilong Donkey Breeding Cooperative (Jinan, Shandong, China); fresh camel milk was purchased from Nierman Trading Co., Ltd. (Hohhot, Inner Mongolia, China); fresh goat milk was sourced from Heqili Family Farm (Xianyang, Shaanxi, China); and fresh cow milk was obtained from Inner Mongolia Yili Industrial Group Co., Ltd. (Hohhot, Inner Mongolia, China). All samples were collected in May 2024. Since fresh milk may be quickly contaminated by microorganisms, we first performed sterilization on all the samples(Li et al., 2024). The five types of fresh milk underwent pasteurization (72–80 °C for 15 s) and were then freeze-dried using a laboratory-scale freeze dryer (Junde FD503, Jinan, Shandong, China). The resulting yak milk powder (YMP), donkey milk powder (DMP), camel milk powder (CMP), goat milk powder (GMP), and cow milk powder (BMP) were collected and stored at −80 °C for subsequent analysis.

2.2. HS-GC-IMS detection

The volatile compounds in the prepared YMP, DMP, CMP, GMP, and BMP samples were detected using a FlavourSpec® gas chromatography-ion mobility spectrometry (G.A.S., Hanon Science Instrument Co., Ltd., Shandong, China). First, 2 g of each YMP, DMP, CMP, GMP, and BMP sample was placed in a 20 mL headspace vial. The samples were then incubated at a headspace temperature of 70 °C with a rotation speed of 500 rpm for 20 min, followed by instrumental analysis. Each sample was measured in triplicate. After 20 min of incubation, 300 μL of sample was injected, with the injection needle temperature maintained at 85 °C. The column used was an MXT-wax capillary column (15 m × 0.53 mm, 1.0 μm, Restek, USA), and the column temperature was set to 60 °C. Nitrogen (N2) gas (purity ≥99.999 %) was used as the carrier gas. The analysis involved a programmed pressure increase: an initial flow rate of 2.00 mL/min for 2 min, linearly increasing to 10.00 mL/min over 8 min, then further increasing to 100.00 mL/min over 10 min, held for 20 min. The total analysis time was 40 min.

The ionization source was a tritium source, with a drift tube length of 53 mm, an electric field strength of 500 V/cm, a drift tube temperature of 45 °C, and a drift gas flow rate of 75 mL/min using high-purity nitrogen gas (purity ≥99.999 %) in positive ion mode. The compounds were characterized using the built-in retention index (RI) database and IMS drift time data in the VOCal 0.4.03 software (G.A.S., Dortmund, Germany). Further analysis with the VOCal data processing software was conducted using Reporter, Gallery Plot, and Dynamic PCA plugins to generate three-dimensional plots, two-dimensional plots, difference spectra, fingerprint spectra, and PCA plots for comparing the volatile compounds between samples(Zhou et al., 2023).

2.3. HS-SPME-GC–MS detection

The separation of volatile compounds in YMP, DMP, CMP, GMP, and BMP samples was conducted using a previously established method with appropriate modifications (F. Zhang, Lu, He, & Yu, 2024). An automatic headspace sampling system was used for extraction, equipped with a 50/30 μm Divinylbenzene/Carboxen/ Polydimethylsiloxane (DVB/CAR/PDMS) extraction fiber (Supelco, Bellefonte, PA, USA) and an MPS2 XL multifunctional autosampler (Gerstel, Germany). A 1.0 g sample was accurately weighed and placed in a 20 mL headspace extraction vial, with an appropriate amount of internal standard solution (5 μg/L ethyl decanoate) added. The sample was then incubated at a constant temperature of 70 °C with shaking for 30 min. Afterward, the extraction fiber was immediately inserted into the vial's headspace for 30 min of extraction. The volatile compounds were then desorbed in the GC–MS injection port (250 °C) for 5 min.

The analysis utilized a GC–MS setup (model 7890 A-5975C, Agilent, USA), featuring a DB-WAXETR capillary column (dimensions: 30 m in length, 0.32 mm internal diameter, and 0.25 μm film thickness, Agilent). For optimal compound detection, the injection port was heated to 250 °C and operated in a splitless mode, allowing all sample components to enter the column. Chromatographic separation was achieved with an oven temperature program: an initial 40 °C hold for 5 min, followed by a 5 °C/min ramp to a final temperature of 250 °C, where it remained for an additional 10 min. Helium was used as the carrier gas, flowing at a rate of 1.7 mL/min.

In the MS system, specific parameters were maintained: the ion source temperature was held at 230 °C, the quadrupole at 150 °C, and the interface at 280 °C. The electron ionization (EI) energy was set to 70 eV, covering a scan range of 35–500 *m/z*. Volatile compounds were identified through comparison with the NIST mass spectral database, achieving a similarity threshold of over 80 %. Additionally, retention indices (RI) of the detected volatile compounds were calculated using an n-alkane (C7–C40) series and matched against established RI values in the database for further confirmation.

2.4. Statistical analysis

All experiments were conducted in triplicate, and the results are presented as mean ± standard deviation (SD). Orthogonal partial least squares discriminant analysis (OPLS-DA) and partial least squares discriminant analysis (PLS-DA) models were performed using OmicStudio tools (https://www.omicstudio.cn/tool). Additionally, hierarchical cluster analysis heatmaps were generated using the heatmap tool (https://www.omicstudio.cn/tool/107) to visually compare the differences in volatile compounds between samples.

3. Results and discussion

3.1. HS-GC-IMS analysis of five milk powder samples

HS-GC-IMS is a simple and convenient method commonly used for detecting flavor compounds in milk and dairy products (Feng et al., 2021a). Notably, HS-GC-IMS is highly sensitive to the detection of alcohols, aldehydes, and ketones (Hu, Wang, Liu, Cao, & Xue, 2021). Fig. 1 presents the 3D spectrum (Fig. 1A), 2D spectrum (Fig. 1B, C), and fingerprint plot (Fig. 1D) of volatile compounds in the five milk powders. In Fig. 1A, the GC-IMS 3D spectra of the five milk powder samples are shown, with the three axes representing drift time (X-axis), retention time (Y-axis), and signal intensity (*Z*-axis). It is clear from Fig. 1A that the volatile compounds in different milk powder samples showed distinct differences, as indicated by the black circled areas, where each sample had its unique peaks. To further visualize the differences in volatile compounds between milk powders, we created a top-down view of the 3D spectra, i.e., the 2D spectra.

Fig. 1B shows the 2D spectra of the five milk powder samples, with the Y-axis representing retention time (s) and the X-axis representing relative drift time (a.u.). The red line at 1.0 on the X-axis marked the normalized reaction ion peak (RIP). The bright spots on either side of the RIP peak represented the volatile compounds, with the colour indicating the concentration of each compound. The colour scale from blue to red indicated increasing compound concentration (Zhou et al., 2023). As shown in Fig. 1B, most signal points appear in the retention time range of 200–1200 s, and the differences in colour and position of the signal points reflect the variation in the types and concentrations of volatile compounds in the milk powder samples.

To further illustrate the distinctions in volatile compounds among the different milk powder samples, we generated a comparative plot based on the 2D spectral data from Fig. 1B, which is presented in Fig. 1C. In this analysis, the 2D spectrum of the YMP sample was set as the reference baseline, and the spectra of DMP, CMP, GMP, and BMP were compared accordingly. For any volatile compounds that matched those found in the YMP sample, the background remained clear, without the blue overlay. When compounds in the other samples differed from YMP, red spots signified higher concentrations relative to the reference, while blue spots indicated lower concentrations. The intensity of each colour reflects the degree of concentration difference: a deeper shade corresponds to a more pronounced variation. As shown in Fig. 1C, the volatile compound profiles among the milk powder samples exhibited considerable diversity.

To accurately identify which volatile compounds exhibited significant differences between the milk powders, we used the Gallery Plot function in the VOCal software to generate a fingerprint plot of the volatile compounds, as shown in Fig. 1D. In Fig. 1D, the columns represent the different milk powder samples, and the rows represented the identified volatile compounds. Each row corresponded to signal peaks identified in different milk powder samples, while each column represented the same volatile compound across different samples. Each point in Fig. 1D represents a volatile compound, and the colour intensity indicated the concentration level. The monomer and dimer forms of the same compound were labelled as M and D, respectively. Due to the incomplete IMS database, two unidentified volatile compounds were marked as “1” and “2” in the fingerprint plot.

From Fig. 1D, it is evident that YMP contains higher levels of methyl acetate, 1-penten-3-ol, 2-pentyl furan, 1-hydroxypropan-2-one, nonanal, 3-penten-2-one, heptanal, propyl acetate, anisole, butyl acetate, pentanal, propionaldehyde, pentan-2-one, 3-hydroxy-2-butanone, p-cymene, and ethyl acetate (as shown in the green box). DMP contains higher levels of 1-butanol, 2,6-dimethylpyrazine, 4-methyl-3-penten-2-one, butyl isobutyrate, 1-propanol, and hexanal (red box). BMP contains higher levels of (E)-2-pentenal, ethyl crotonate, propan-2-ol, 4-methyl-2-pentanone, heptan-2-one, and butan-2-one (yellow box).

Previous studies had analysed the flavor compounds in milk using methods such as GC–MS and GC-O-MS (Jo, Benoist, Barbano, & Drake, 2018; Xi et al., 2024). HS-GC-IMS has also been reported for investigating the flavor compounds in cow's milk, camel milk, and yak milk (Yang et al., 2023; Zhao et al., 2023). Our previous research employed the HS-GC-IMS method to detect differences in the volatile compounds of yak milk powder under different sterilization and drying conditions

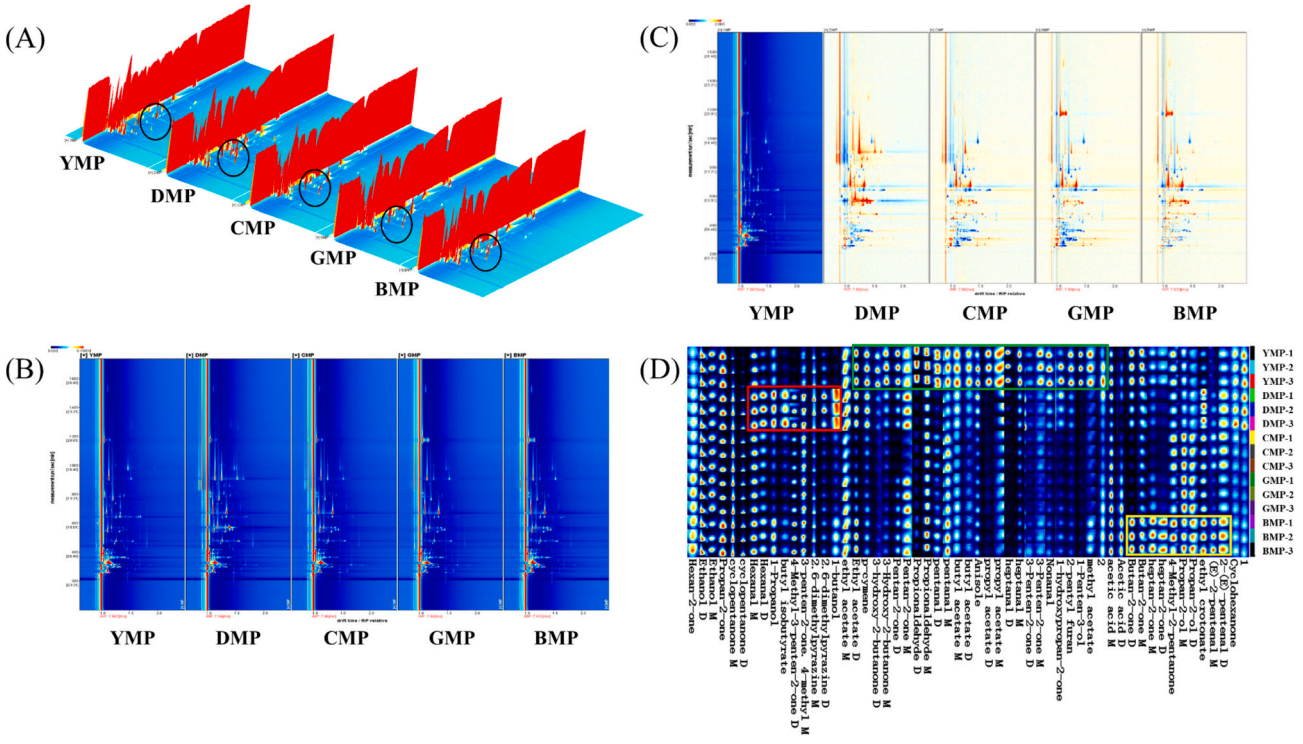

Fig. 1. GC-IMS spectra of volatile compounds in five milk powders. 3D spectra (Fig. 1A), 2D spectra (Fig. 1B, C), and fingerprint plot (Fig. 1D).

(Feng et al., 2021a, 2021). The successful application of these studies demonstrates that HS-GC-IMS is well-suited for the analysis of flavor compounds in milk powder. The results in Fig. 1 further confirm the variations in flavor compounds among the five different types of milk powders.

3.2. Identification and analysis of volatile compounds in HS-GC-IMS

In the HS-GC-IMS detection process, volatile compounds in the milk powder samples were identified using the GC × IMS Library Search, which employed a two-dimensional cross-qualitative approach. The annotated 2D spectra for each sample are presented in Fig. 2A. On this graph, the x-axis displayed the drift time of detected compounds, while the y-axis showed their retention time. Identified volatile compounds were marked with red numbers, each corresponding to entries in Table 1. Table 1 provided a comprehensive breakdown of the 55 volatile compounds detected across the five milk powder samples, aligning the numbered annotations in Fig. 2A with detailed compound information. This dual reference between Fig. 2A and Table 1 highlights the distribution and diversity of volatile compounds in the milk powders analysed.

Additionally, since dimeric forms of compounds had a stronger proton affinity, their drift time was longer than their monomeric counterparts during detection (Lantsuzskaya, Krisilov, & Levina, 2015). The concentration of dimers and monomers also differed, which resulted in two signals for the same compound (M. Li et al., 2019). In our experiment, 17 compounds were detected in both monomeric and dimeric forms, including propyl acetate, propionaldehyde, propan-2-ol, pentanal, pentan-2-one, hexanal, heptanal, heptan-2-one, ethyl acetate, ethanol, cyclopentanone, butyl acetate, butan-2-one, acetic acid, 4-methyl-3-penten-2-one, 3-penten-2-one, 3-hydroxy-2-butanone, and 2.6-dimethylpyrazine. Both the monomer and dimer forms of each compound were counted separately. Ultimately, 55 compounds were detected in the milk powder samples, with 53 compounds successfully identified.

The aroma of milk powder primarily depended on the types and concentrations of volatile compounds present. Previous studies found that the volatile compound profiles in yak milk varied based on the collection period, processing methods, and storage conditions (Feng et al., 2021; Yang et al., 2023; Zhang, Zhong, et al., 2024). Therefore, the differences in the types and concentrations of volatile compounds in different milk powders directly led to variations in their aroma. Fig. 2B shows the distribution of various types of volatile compounds in the five milk powder samples. This figure is based on the peak volumes of each volatile compound, which were directly proportional to their concentration (Feng et al., 2021a). It was evident that the identified volatile compounds mainly included ketones, alcohols, aldehydes, acids, pyrazines, esters, terpenes, ethers, and a small number of furans. The figure clearly shows that the DMP and YMP samples contained the highest concentrations of ketones and esters, which were likely the main reasons for the significant differences in volatile compounds between DMP, YMP, and the other three samples.

3.3. PCA and hierarchical clustering analysis of volatile compounds identified by HS-GC-IMS

To better distinguish the variations in volatile compounds among the milk powder samples, we conducted PCA and hierarchical clustering heatmap analyses on the 85 volatile compounds identified through HS-GC-IMS. Fig. 3A and B illustrate the PCA results: Fig. 3A displays a two-dimensional PCA plot, while Fig. 3B shows a three-dimensional representation. In Fig. 3A, PC1 explained 47 % of the variance, and PC2 accounted for 25 %, with a combined contribution of 72 %, indicating that these two components effectively captured the primary characteristics of the samples.

The positioning of sample points in Fig. 3A demonstrates that DMP and YMP were significantly separated from the other samples, while GMP, CMP, and BMP appeared closely grouped. This clustering indicated that the volatile compound profiles of GMP, CMP, and BMP were quite similar, whereas DMP and YMP exhibited distinctive differences. These results underscored notable variations in aroma composition among the samples, particularly highlighting DMP and YMP as having the most unique profiles.

Hierarchical clustering heatmap analysis, a frequently used method for grouping samples, visually represented the relationships among the milk powder samples based on proximity (W. Li, Wang, Sun, & Bahrami, 2023). Previous research has successfully applied hierarchical clustering heatmaps to highlight differences in volatile compound profiles(Sun, Lin, Li, & Li, 2024). Fig. 3C illustrates these results, with colour intensity indicating the relative content of volatile compounds: darker red squares represent higher compound concentrations, while paler squares denote lower levels. This colour gradient effectively visualizes peak intensity, highlighting compositional differences among the milk powders (Chen et al., 2021). The heatmap analysis uncovered distinct profiles among the five samples, with each sample initially forming a separate cluster. As clustering progressed, CMP and GMP grouped first, followed sequentially by BMP, DMP, and YMP. This clustering order (CMP > GMP > BMP > DMP > YMP) reflects the relative similarities in volatile composition across the samples.

3.4. OPLS-DA and PLS-DA of volatile compounds identified by HS-GC-IMS

Multivariate statistical analysis can explore the interdependencies among multiple variables and underlying statistical patterns. By utilizing multivariate statistics, complex datasets can be managed, helping to reveal relationships between samples and the contributions of specific variables (Chen et al., 2024). OPLS-DA and PLS-DA are commonly used multivariate statistical methods in food flavor research (Herbert-Pucheta, Lozada-Ramírez, Ortega-Regules, Hernández, & Anaya de Parrodi, 2021). PLS-DA combines PLS regression with discriminant analysis, allowing for both the prediction of sample categories and the identification of each variable (flavor compound) contributing to the classification results. This aids in discovering components closely related to specific flavor characteristics (Shi et al., 2023). OPLS-DA is an improved version of PLS-DA. It not only facilitates sample classification but also separates noise or interference signals unrelated to classification from systematic differences related to classification, thereby enhancing the model's interpretability and reliability (Ping et al., 2024).

We performed an OPLS-DA analysis on the HS-GC-IMS data from the five milk powder samples, with the results illustrated in Fig. 4A and B. As shown in Fig. 4A, the sample points for each milk powder were distinctly separated, with YMP and BMP clustering in the third and fourth quadrants, respectively. The OPLS-DA model demonstrated strong predictive reliability, as reflected by the model parameters R^2 (0.979) and Q^2 (0.942), indicating a high degree of model accuracy (Cheng et al., 2021). To verify if the model was overfitting, we conducted 200 permutation tests, as shown in Fig. 4B. After 200 cross-validations, the regression line for the model Q2 crossed the horizontal axis, with the original Q^2 and R^2 values consistently higher than all Q^2 and R^2 values from the permutation tests. Both the R^2 and Q^2 regression line slopes were greater than 1, and the intercept for the Q2 regression line was negative (−0.6565). These results suggested that the OPLS-DA model was not overfitting, and its predictive capability was valid (Qi, Ding, Pan, Li, & Fu, 2020).

Additionally, we performed a PLS-DA analysis on the HS-GC-IMS data, with results shown in Fig. 4C and D. Like the OPLS-DA results, the PLS-DA results also showed that the sample points for YMP and BMP were distant from the other samples. DMP, CMP, and GMP sample points did not overlap either. Moreover, the permutation test confirmed that the PLS-DA model was reliable (Fig. 4D). These results indicated that the volatile components detected by HS-GC-IMS effectively differentiate between the different milk powders.

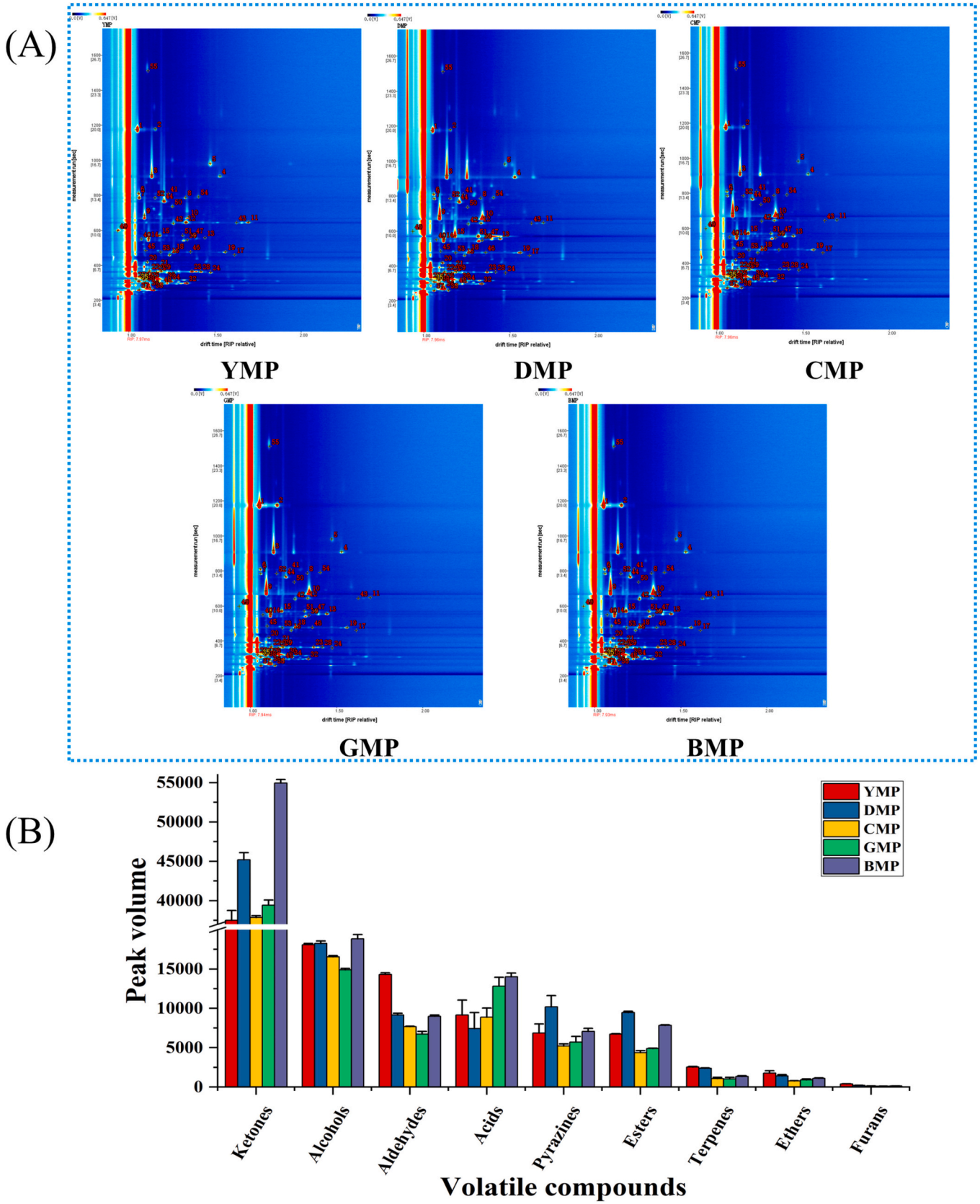

Fig. 2. Identification and analysis results of volatile compounds in different milk powder samples. (A) Library search qualitative analysis. (B) Relative content of various volatile compounds (calculated based on peak volume).

Table 1
Volatile compounds identified from five milk powder samples using HS-GC-IMS.

Count	Compound	CAS#	Formula	MW	RI	Rt [*sec*]	Dt [a.u.]	Comment
1	acetic acid M	C64197	C2H4O2	60.1	1487.0	1172.922	1.04897	spicy
2	Acetic acid D	C64197	C2H4O2	60.1	1489.4	1178.763	1.15741	spicy
3	2,6-dimethylpyrazine M	C108509	C6H8N2	108.1	1370.3	917.868	1.13458	roast, coffee, peanut, potato
4	2,6-dimethylpyrazine D	C108509	C6H8N2	108.1	1366.2	910.08	1.53218	roast, coffee, peanut, potato
5	Nonanal	C124196	C9H18O	142.2	1402.5	982.118	1.47321	rose, citrus, strong oily
6	Anisole	C100663	C7H8O	108.1	1311.5	811.171	1.06054	anise
7	3-Hydroxy-2-butanone M	C513860	C4H8O2	88.1	1295.7	784.668	1.06209	butter, cream
8	3-hydroxy-2-butanone D	C513860	C4H8O2	88.1	1296.4	785.82	1.33219	butter, cream
9	cyclopentanone M	C120923	C5H8O	84.1	1222.8	684.417	1.09314	pleasant
10	cyclopentanone D	C120923	C5H8O	84.1	1215.5	675.198	1.34927	pleasant
11	heptanal D	C111717	C7H14O	114.2	1193.2	647.543	1.69853	fresh, aldehyde, fatty, green herbs, wine, fruity
12	heptanal M	C111717	C7H14O	114.2	1190.4	642.933	1.33374	fresh, aldehyde, fatty, green herbs, wine, fruity
13	4-Methyl-3-penten-2-one D	C141797	C6H10O	98.1	1145.1	557.662	1.44395	spice, earth, green
14	3-penten-2-one, 4-methyl M	C141797	C6H10O	98.1	1141.2	550.749	1.11953	spice, earth, green
15	ethyl crotonate	C623701	C6H10O2	114.1	1152.9	571.36	1.18312	sourness, fruity, rum ether
16	butyl acetate M	C123864	C6H12O2	116.2	1081.9	459.884	1.24038	fruity
17	butyl acetate D	C123864	C6H12O2	116.2	1081.9	459.884	1.61651	fruity
18	Hexanal M	C66251	C6H12O	100.2	1098.6	481.814	1.26733	fresh, green, fat, fruity
19	Hexanal D	C66251	C6H12O	100.2	1094.6	476.331	1.56486	fresh, green, fat, fruity
20	1-Propanol	C71238	C3H8O	60.1	1048.2	419.14	1.11052	alcohol, pungent
21	4-Methyl-2-pentanone	C108101	C6H12O	100.2	1022.8	390.811	1.17848	ketone
22	Pentan-2-one M	C107879	C5H10O	86.1	1000.0	366.955	1.12272	acetone, fresh, sweet fruity, wine
23	Pentan-2-one D	C107879	C5H10O	86.1	999.6	366.583	1.3693	acetone, fresh, sweet fruity, wine
24	propyl acetate D	C109604	C5H10O2	102.1	990.6	359.128	1.47822	fruity, pear
25	propyl acetate M	C109604	C5H10O2	102.1	991.7	359.873	1.16454	fruity, pear
26	Ethanol D	C64175	C2H6O	46.1	932.3	319.99	1.12272	aromaticity
27	Ethanol M	C64175	C2H6O	46.1	933.5	320.735	1.0443	aromaticity
28	pentanal D	C110623	C5H10O	86.1	998.2	365.199	1.4196	green grassy, faint banana, pungent
29	pentanal M	C110623	C5H10O	86.1	999.3	366.307	1.19101	green grassy, faint banana, pungent
30	Propan-2-ol D	C67630	C3H8O	60.1	932.9	320.33	1.21741	alcohol, spicy
31	Propan-2-ol M	C67630	C3H8O	60.1	930.8	319.037	1.08863	alcohol, spicy
32	Ethyl acetate D	C141786	C4H8O2	88.1	896.9	298.357	1.33976	fresh, fruity, sweet, grassy
33	ethyl acetate M	C141786	C4H8O2	88.1	902.9	301.865	1.09764	fresh, fruity, sweet, grassy
34	Butan-2-one D	C78933	C4H8O	72.1	913.6	308.328	1.24639	fruity, camphor
35	Butan-2-one M	C78933	C4H8O	72.1	915.3	309.374	1.06118	fruity, camphor
36	Propan-2-one	C67641	C3H6O	58.1	852.9	273.461	1.1228	fresh, apple, pear
37	Propionaldehyde M	C123386	C3H6O	58.1	827.0	259.78	1.06314	pungent, green grassy
38	Propionaldehyde D	C123386	C3H6O	58.1	826.1	259.352	1.14639	pungent, green grassy
39	3-Penten-2-one D	C625332	C5H8O	84.1	1138.2	545.679	1.34164	Fruity, turns into spicy during storage
40	3-Penten-2-one M	C625332	C5H8O	84.1	1140.5	549.54	1.07583	Fruity, turns into spicy during storage
41	1-hydroxypropan-2-one	C116096	C3H6O2	74.1	1310.8	810.111	1.23225	pungent, caramel, fresh
42	heptan-2-one M	C110430	C7H14O	114.2	1188.6	639.292	1.26088	pear, banana, fruity, slight medicinal fragrance
43	heptan-2-one D	C110430	C7H14O	114.2	1190.1	642.187	1.62892	pear, banana, fruity, slight medicinal fragrance
44	p-cymene	C99876	C10H14	134.2	1284.7	768.612	1.20567	fresh citrus terpene woody spice
45	(*E*)-2-pentenal M	C1576870	C5H8O	84.1	1099.7	483.458	1.09979	potato, peas
46	2-(E)-pentenal D	C1576870	C5H8O	84.1	1094.8	476.582	1.36125	potato, peas
47	1-butanol	C71363	C4H10O	74.1	1152.0	569.752	1.38102	wine
48	methyl acetate	C79209	C3H6O2	74.1	888.1	293.213	1.19477	ethereal
49	1-Penten-3-ol	C616251	C5H10O	86.1	1166.9	597.125	0.93838	ethereal, green, tropical fruity
50	2-pentyl furan	C3777693	C9H14O	138.2	1261.4	735.796	1.25632	bean, fruity, earthy, green, vegetable
51	butyl isobutyrate	C97870	C8H16O2	144.2	1152.7	571.103	1.316	fruity, sweet
52	Cyclohexanone	C108941	C6H10O	98.1	1295.3	784.106	1.15539	strong pungent, earthy
53	Hexan-2-one	C591786	C6H12O	100.2	1093.6	474.907	1.18764	fruity, fungal, meaty, buttery
54	1	unidentified	*	0	1299.6	791.169	1.40858	
55	2	unidentified	*	0	1607.5	1510.657	1.11468	

Note: The suffixes M and D represent the monomer and dimer forms of the same compound, respectively. Numbers indicate unidentified peaks. The descriptions of the substances' odors were primarily referenced from the https://www.flavornet.org, https://www.femaflavor.org, and https://www.chemicalbook.com databases. MW: molecular mass. RI: the retention index (experimental value). Rt [sec]: the retention time. Dt [a.u.]: the drift time.

Furthermore, based on the OPLS-DA results, we screened for key volatile compounds identified by HS-GC-IMS, as shown in Fig. 5. Fig. 5A displays the Variable Importance in Projection (VIP) scores, with detailed VIP values for various volatile compounds provided in Table S2. The VIP scores from the OPLS-DA results can identify the main differences between samples (Ye, Wang, Zhan, Tian, & Liu, 2022). Fig. 5A shows that out of the 55 volatile compounds identified by HS-GC-IMS, 27 had VIP > 1 and $p < 0.05$. We considered these compounds as potentially significant volatile compounds differentiating the five milk powders. We further performed a hierarchical clustering heatmap analysis on these 27 key volatile compounds (Fig. 5B). The results in Fig. 5B indicated that YMP had higher levels of 17 compounds compared to other milk powder samples. YMP and DMP had similar types and amounts of volatile compounds, while BMP, GMP, and CMP had comparable types and amounts of volatile compounds.

In conclusion, the HS-GC-IMS results showed significant differences in the volatile compounds among the five milk powder samples. The 3D and 2D spectra revealed unique peaks for each sample, reflecting differences in the types and concentrations of volatile compounds. However, HS-GC-IMS had some limitations in quantification, and its quantitative results were not as accurate as those of HS-SPME-GC–MS (Song & Liu, 2018). Therefore, we further employed HS-SPME-GC–MS to measure and analyse the volatile compounds in the five milk powder samples.

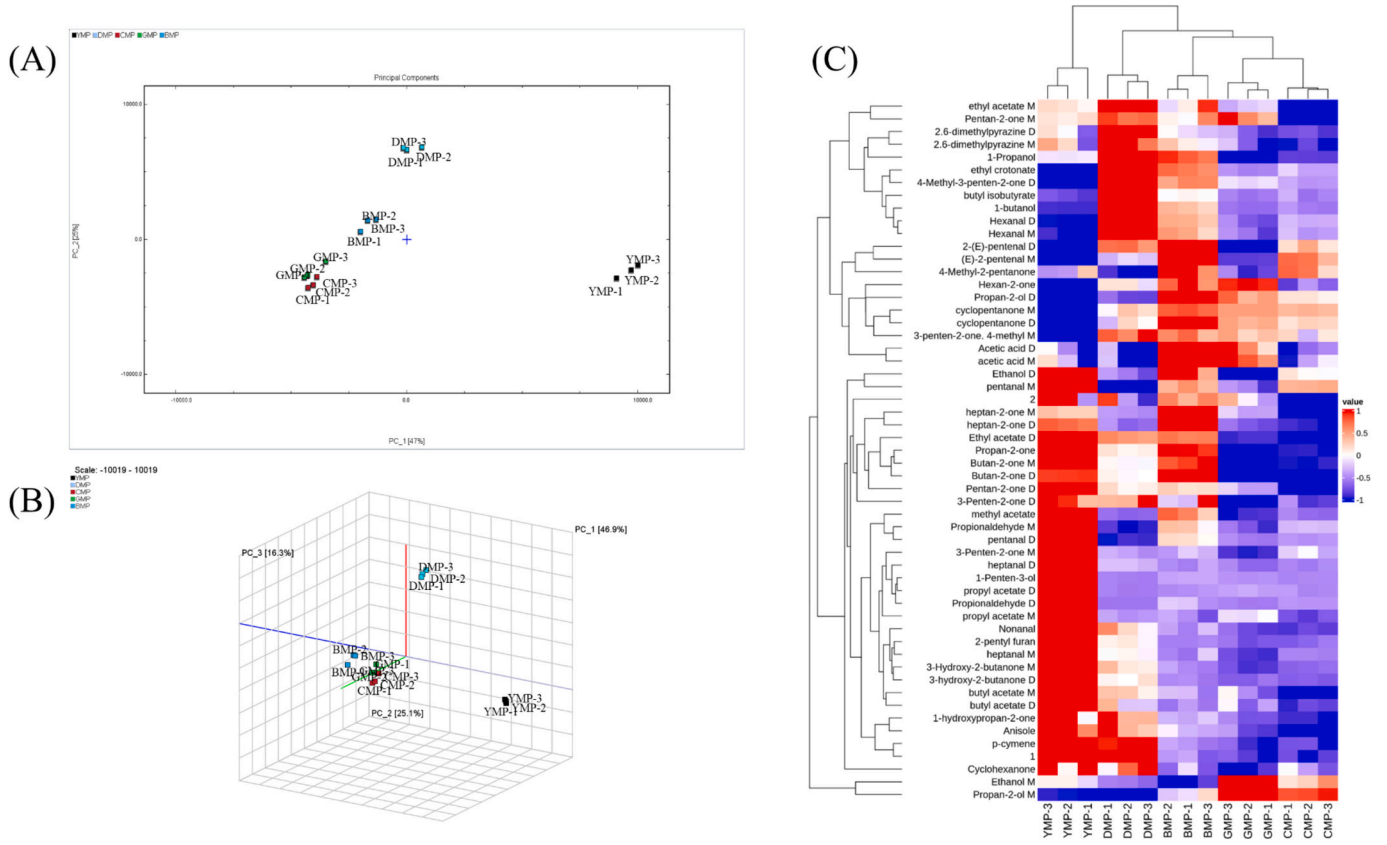

Fig. 3. PCA and hierarchical clustering analysis of volatile compounds identified using HS-GC-IMS. (A) 2D PCA plot. (B) 3D PCA plot. (C) Hierarchical clustering heatmap.

3.5. HS-SPME-GC–MS analysis of the five milk powder samples

HS-SPME-GC–MS has become a prominent tool in food flavor research, frequently used to analyse volatile compounds in dairy products (Chi et al., 2021; Pan et al., 2019). Consequently, we employed HS-SPME-GC–MS to further analyse volatile compounds in the five milk powder samples. Fig. S1 presents the total ion chromatograms, highlighting variations in peak times, intensities, and volumes across the samples. Table 2 summarized the identified volatile compounds, with a total of 86 compounds detected. Of these, 15 compounds were found in all milk powders (Fig. 6A), while DMP, YMP, CMP, GMP, and BMP exhibited unique volatile profiles, containing 24, 7, 4, 1, and 1 unique compound, respectively (Fig. 6A). The higher number of unique compounds in DMP and YMP likely contributed to their distinct flavor profiles compared to the others. Fig. 6B displays a stacked bar chart of the relative quantities of each volatile compound, showing that ester compounds were most abundant in YMP and DMP. These esters may serve as key flavor markers that set these two samples apart, consistent with previous HS-GC-IMS findings.

We also conducted a PCA analysis on the HS-SPME-GC–MS data, with the results presented in Fig. 6C. The PCA plot revealed that the first principal component (PC1) accounted for 40.1 % of the variance, while the second principal component (PC2) explained 22.2 %. Together, PC1 and PC2 contributed to 62.3 % of the total variance, indicating that they captured the main variations across the samples. In the plot, DMP and YMP were in the fourth and third quadrants, respectively, while GMP, CMP, and BMP clustered in the second quadrant without any overlap. These findings reinforced the significant differences in the volatile profiles of DMP and YMP compared to GMP, CMP, and BMP, aligning with the previous HS-GC-IMS results and further confirming the distinct differences among the milk powder samples.

We also performed hierarchical clustering heatmap analysis on the HS-SPME-GC–MS data, with the results shown in Fig. 6D. The heatmap revealed distinct differences in the types and distributions of volatile compounds across the five milk powder samples, with each sample exhibiting a unique profile of volatile compounds. Initially, the samples formed separate clusters. As the clustering progressed, CMP and GMP grouped together first, followed by BMP, YMP, and DMP. Thus, the clustering order of volatile compounds among the five milk powder samples based on the HS-SPME-GC–MS data was CMP > GMP > BMP > YMP > DMP. For each type of milk powder, the following volatile compounds are unique to specific milk sources. In yak milk powder, the unique volatile compounds include (Adipic acid, di(but-2-en-1-yl) ester), Methyl formate, Acetoin, (Sulfurous acid, decyl 2-ethylhexyl ester), (Borane, diethyl(decyloxy)-), (Phthalic acid, cyclohexyl isohexyl ester), and Diisobutyl phthalate. In donkey milk powder, the specific compounds detected include 5-Ethylcyclopent-1-enecarboxaldehyde, Propargyl alcohol, (Furan, 2-propyl-), (Dodecane, 2,6,10-trimethyl-), ethyl decanoate, pentanol, (Phthalic acid, 6-ethyl-3-octyl butyl ester), (Heptanoic acid, 2-ethyl-), Ethyl laurate, Nonanal, hexanal, heptanol, 1-Hexen-3-ol, 1-octen-3-ol, Ethyl octanoate, and 1-Hepten-3-one. In camel milk powder, the specific compounds detected include (1H-Pyrazole, 3-ethyl-4,5-dihydro-), (5,5-Dibutylnonane), (1-Pentene, 4,4-dimethyl-), Myristic acid, and Lauric acid. In goat milk powder, the unique compound is Toluene. In cow milk powder, the unique compound is 6-ethyl-Undecane.

3.6. OPLS-DA and PLS-DA of volatile compounds identified by HS-SPME-GC–MS

As in the previous analysis, we applied OPLS-DA and PLS-DA to the volatile compounds identified by HS-SPME-GC–MS, with the results presented in Fig. 7. Fig. 7A shows the OPLS-DA score plot, which clearly demonstrates the distinct distribution of the milk powder samples. DMP

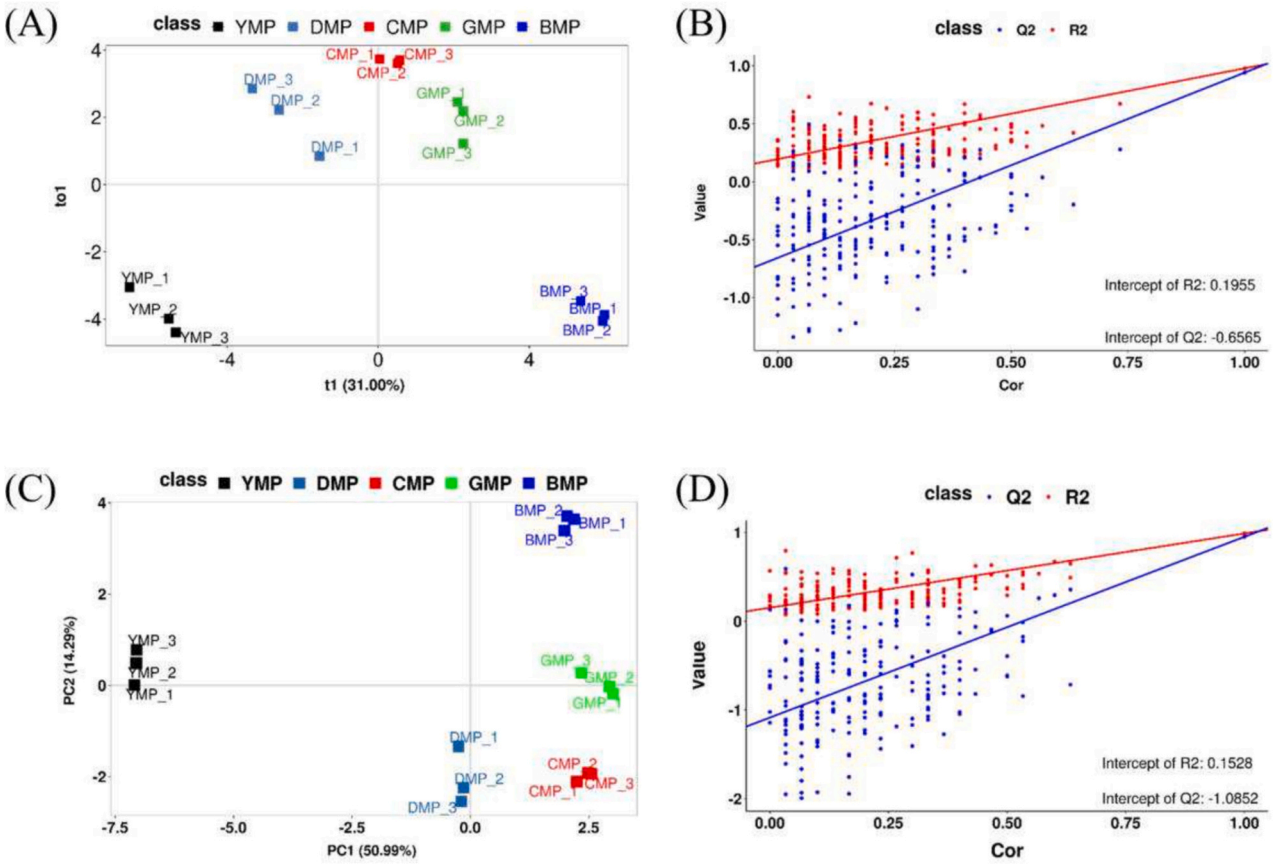

Fig. 4. OPLS-DA and PLS-DA results of volatile compounds identified by HS-GC-IMS. (A) OPLS-DA score plot. (B) OPLS-DA model validation plot (after 200 permutation tests). (C) PLS-DA score plot. (D) PLS-DA model validation plot (after 200 permutation tests).

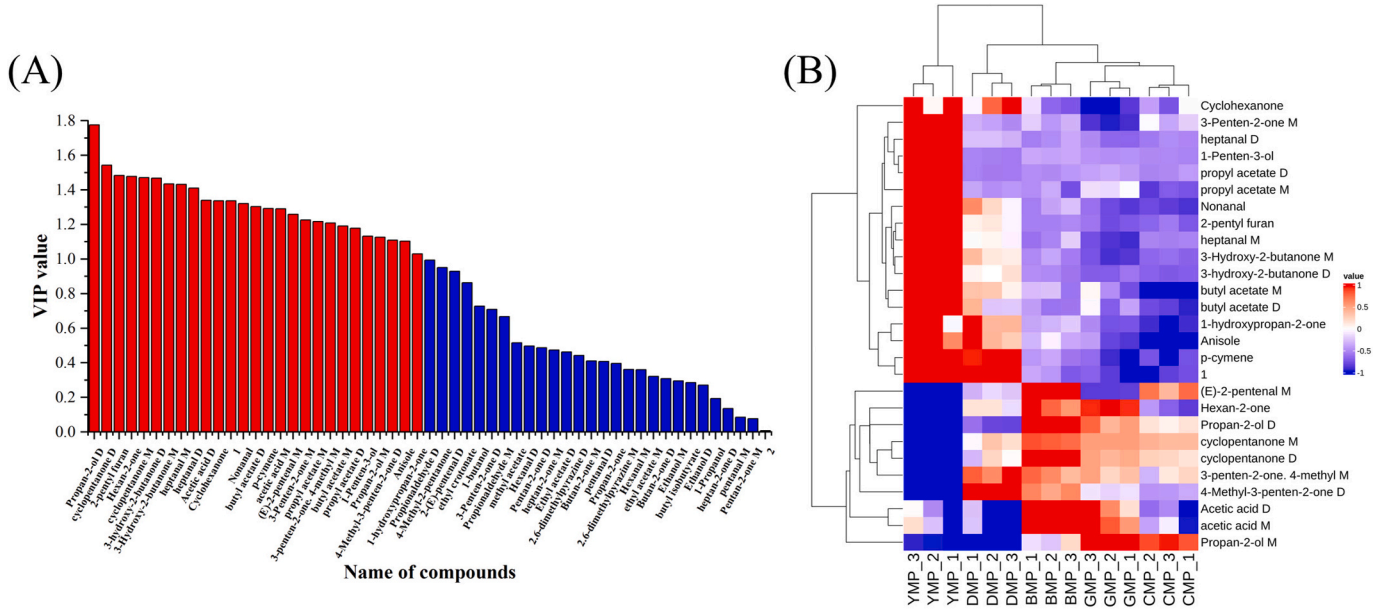

Fig. 5. Screening of key volatile compounds identified by HS-GC-IMS. (A) VIP score plot (based on OPLS-DA results). (B) Hierarchical clustering heatmap analysis of key volatile compounds.

and YMP were positioned farthest from the other samples, located in the second and third quadrants, respectively. The OPLS-DA model yielded an R2 of 0.986 and a Q2 of 0.933 (Table S1), indicating excellent predictive capability. In Fig. 7B, the 200 permutation tests for the OPLS-DA model confirmed that there was no overfitting. Additionally, the PLS-DA analysis results (Fig. 7C and D) further supported the significant differences in volatile compounds among the five milk powders, with the permutation tests confirming a strong model fit.

Table 2
Volatile compounds identified from five milk powder samples using HS-SPME-GC–MS.

Number	Retention time (min)	Compound name	CAS ID	YMP	DMP	CMP	GMP	BMP
1	4.267	Dimethyl ether	115–10-6	3593 ± 1239	2743 ± 714	13,607 ± 1167	10,886 ± 6255	9660 ± 985
2	6.307	toluene	108–88-3	ND	ND	ND	1382 ± 149	ND
3	7.575	hexanal	66–25-1	ND	622 ± 75	ND	ND	ND
4	7.868	3,4-Hexanedione, 2,2,5-trimethyl-	20,633–03-8	ND	ND	169 ± 39	ND	236 ± 8
5	9.218	Propargyl alcohol	107–19-7	ND	16.6 ± 0.8	ND	ND	ND
6	9.252	3,3-Diethoxy-1-propyne	10,160–87-9	19.6 ± 7.0	21.1 ± 0.3	ND	ND	ND
7	9.848	Pentane, 2,3-dimethyl-	565–59-3	ND	38.0 ± 2.3	ND	ND	ND
8	10.962	dodecane	112–40-3	192 ± 8	101 ± 3	225 ± 9	367 ± 45	219 ± 4
9	11.645	Propanoic acid, 2-hydroxy-2-methyl-, ethyl ester	80–55-7	ND	ND	330 ± 22	321 ± 6	187 ± 11
10	12.237	Ethyl caproate	123–66-0	ND	55.8 ± 10.3	ND	ND	150 ± 11
11	12.803	styrene	100–42-5	ND	ND	203 ± 10	290 ± 9	178 ± 21
12	13.011	pentanol	71–41-0	ND	31.9 ± 4.8	ND	ND	ND
13	13.565	2-Butanone, 3-ethoxy-3-methyl-	36,687–99-7	56.9 ± 5.7	60.0 ± 8.6	ND	417 ± 25	270 ± 26
14	14.247	1-Hepten-3-one	2918-13-0	ND	9.82 ± 1.02	ND	ND	ND
15	14.902	(E)-2-heptenal	18,829–55-5	ND	78.0 ± 10.0	ND	ND	ND
16	14.92	Cyclopentane, 1,1-dimethyl-	1638–26-2	ND	79.6 ± 17.0	ND	ND	ND
17	15.005	Ethyl 4-(ethyloxy)-2-oxobut-3-enoate	1,000,305–38-2	ND	70.0 ± 14.4	ND	ND	ND
18	15.778	Tetradecane, 2,2-dimethyl-	59,222–86-5	48.9 ± 1.9	16.3 ± 0.5	ND	ND	ND
19	16.279	2-hydroxy-2-methyl-4-pentanone	123–42-2	13.6 ± 2.2	45.7 ± 6.1	271 ± 7	356 ± 60	195 ± 10
20	16.657	Undecane, 4,7-dimethyl-	17,301–32-5	ND	ND	190 ± 11	254 ± 40	152 ± 4
21	16.662	tetradecane	629–59-4	175 ± 8	102 ± 5	198 ± 10	244 ± 34	ND
22	16.742	Nonanal	124–19-6	ND	54.8 ± 43.6	ND	ND	ND
23	17.239	3-Octen-2-one	1669-44-9	ND	46.0 ± 2.5	ND	ND	ND
24	17.352	5-Ethylcyclopent-1-enecarboxaldehyde	36,431–60-4	ND	12.0 ± 0.1	ND	ND	ND
25	17.805	Sulfurous acid, decyl 2-ethylhexyl ester	1,000,309–19-3	34.2 ± 2.5	ND	ND	ND	ND
26	17.811	3-Ethyl-2,6,10-trimethylundecane	1,000,432–25-9	35.2 ± 0.1	ND	281 ± 8	341 ± 46	126 ± 11
27	17.815	Borane, diethyl(decyloxy)-	1,000,152–34-3	34.7 ± 0.7	ND	ND	ND	ND
28	17.818	Ethyl octanoate	106–32-1	ND	872 ± 147	ND	ND	ND
29	18.165	Tetradecane, 2-methyl-	6418-41-3	ND	12.9 ± 0.6	79.6 ± 9.7	115 ± 26	28.3 ± 5.6
30	18.387	Tetradecane, 3-methyl-	18,435–22-8	15.8 ± 0.9	ND	159 ± 19	198 ± 21	64.8 ± 3.2
31	18.407	5,5-Dibutylnonane	6008-17-9	ND	ND	169 ± 16	ND	ND
32	18.451	1-octen-3-ol	3391-86-4	ND	83.9 ± 9.6	ND	ND	ND
33	18.458	1-Hexen-3-ol	4798-44-1	ND	75.9 ± 1.7	ND	ND	ND
34	18.608	heptanol	111–70-6	ND	7.60 ± 1.97	ND	ND	ND
35	18.83	acetic acid	64–19-7	76.1 ± 15.9	ND	212 ± 24	274 ± 39	153 ± 3
36	19.281	pentadecane	629–62-9	260 ± 26	535 ± 21	3542 ± 174	3963 ± 241	1502 ± 138
37	19.446	2-ethylhexanol	104–76-7	65.5 ± 9.0	94.2 ± 7.2	145 ± 36	186 ± 23	120 ± 9
38	19.447	1-Pentene, 4,4-dimethyl-	762–62-9	ND	ND	180 ± 6	ND	ND
39	19.535	Furan, 2-propyl-	4229-91-8	ND	19.9 ± 0.7	ND	ND	ND
40	20.103	Decane, 3-ethyl-3-methyl-	17,312–66-2	ND	21.4 ± 3.7	ND	88.0 ± 6.1	53.9 ± 4.1
41	20.659	Pentadecane, 2-methyl-	1560-93-6	ND	63.7 ± 7.0	500 ± 101	370 ± 86	146 ± 20

(*continued on next page*)

Table 2 (*continued*)

Number	Retention time (min)	Compound name	CAS ID	YMP	DMP	CMP	GMP	BMP
42	20.896	Pentadecane, 3-methyl-	2882-96-4	43.1 ± 2.5	77.0 ± 0.9	389 ± 23	312 ± 42	144 ± 4
43	21.709	Hexadecane	544–76-3	178 ± 8	650 ± 37	4065 ± 328	3290 ± 77	1612 ± 176
44	21.975	2,3-Butanediol, [S-(R*,R*)]-	19,132–06-0	ND	53.3 ± 4.8	194 ± 8	ND	ND
45	22.243	Sulfurous acid, dodecyl 2-ethylhexyl ester	1,000,309–19-5	38.5 ± 3.0	ND	ND	ND	ND
46	22.278	Pentadecane, 2,6,10-trimethyl-	3892-00-0	37.7 ± 6.0	232 ± 18	920 ± 66	587 ± 91	298 ± 27
47	22.518	Undecane, 6-ethyl-	17,312–60-6	ND	ND	ND	ND	116 ± 29
48	22.543	Hexadecane, 7-methyl-	26,730–20-1	ND	79.4 ± 12.5	ND	224 ± 24	114 ± 31
49	22.569	Pentadecane, 6-methyl-	10,105–38-1	ND	67.1 ± 11.6	ND	ND	ND
50	22.772	ethyl decanoate	110–38-3	ND	268 ± 47	ND	ND	ND
51	22.976	Tetradecane, 1-iodo-	19,218–94-1	ND	29.0 ± 8.6	ND	76.9 ± 10.1	ND
52	22.997	butyric acid	107–92-6	295 ± 10	ND	555 ± 19	269 ± 70	2520 ± 225
53	23.024	Methyl formate	107–31-3	294 ± 14	ND	ND	ND	ND
54	23.407	2,6,10,14-Tetramethylpentadecane	1921-70-6	ND	185 ± 18	465 ± 45	283 ± 26	188 ± 40
55	23.618	Pentanoic acid, 2-methyl-, anhydride	63,169–61-9	ND	45.6 ± 4.6	ND	ND	ND
56	23.774	2-Butanol, 1-methoxy-	53,778–73-7	ND	ND	ND	ND	68.0 ± 5.6
57	23.939	Heptadecane	629–78-7	24.5 ± 1.8	387 ± 41	942 ± 96	625 ± 48	360 ± 45
58	24.415	E,E-2,4-Nonadienal	5910-87-2	ND	53.7 ± 3.3	ND	ND	ND
59	25.686	Dodecane, 2,6,10-trimethyl-	3891-98-3	ND	25.7 ± 2.7	ND	ND	ND
60	26.095	octadecane	593–45-3	ND	60.6 ± 10.2	ND	ND	ND
61	26.704	Ethoxyacetylene	927–80-0	ND	ND	ND	36.1 ± 2.1	87.7 ± 5.0
62	26.712	1-Oxa-3,4-diazacyclopentadiene	288–99-3	12.6 ± 0.8	ND	ND	ND	84.4 ± 7.5
63	27.224	Ethyl laurate	106–33-2	ND	47.9 ± 4.9	ND	ND	ND
64	27.682	Pentanoic acid	109–52-4	219 ± 5	ND	ND	244 ± 77	ND
65	27.683	caproic acid	142–62-1	228 ± 6	302 ± 8	1891 ± 115	243 ± 71	1891 ± 162
66	28.331	phenylmethanol	100–51-6	ND	30.9 ± 1.9	73.9 ± 7.1	94.3 ± 8.7	71.5 ± 3.4
67	28.705	2,4,6-Tris(1,1-dimethylethyl)-4-methylcyclohexa-2,5-dien-1-one	19,687–22-0	ND	ND	94.2 ± 8.8	80.3 ± 7.7	ND
68	29.134	dimethyl sulphone	67–71-0	264 ± 10	41.0 ± 3.9	371 ± 29	444 ± 71	305 ± 18
69	29.899	1-Decanol	112–30-1	ND	7.59 ± 1.30	51.9 ± 17.9	38.6 ± 4.6	ND
70	30.247	Hexanoic acid, 1,1-dimethylpropyl ester	116,423–69-9	ND	6.99 ± 0.53	ND	ND	33.9 ± 1.6
71	30.642	Acetoin	513–86-0	3.11 ± 0.54	ND	ND	ND	ND
72	31.863	octanoic acid	124–07-2	38.6 ± 1.5	290 ± 72	837 ± 75	118 ± 15	641 ± 60
73	33.497	Ethanol, 2-phenoxy-	122–99-6	421 ± 37	357 ± 9	1060 ± 64	1309 ± 165	678 ± 34
74	34.441	2H-Pyran-2-one, tetrahydro-6-propyl-	698–76-0	18.3 ± 3.0	11.7 ± 1.4	ND	45.2 ± 10.7	103 ± 6
75	35.031	Heptanoic acid, 2-ethyl-	3274-29-1	ND	4.74 ± 0.57	ND	ND	ND
76	35.313	Adipic acid, di(but-2-en-1-yl) ester	1,000,324–71-1	20.0 ± 2.5	ND	ND	ND	ND
77	35.672	decanoic acid	334–48-5	11.1 ± 5.3	18.8 ± 3.5	267 ± 28	35.4 ± 7.3	181 ± 42
78	36.262	Pentanoic acid, 5-hydroxy-, 2,4-di-t-butylphenyl esters	166,273–38-7	ND	15.6 ± 1.2	54.6 ± 1.6	ND	ND
79	38.476	2-Chloroethyl benzoate	939–55-9	29.2 ± 2.1	3.90 ± 0.85	41.6 ± 7.8	48.6 ± 13.9	28.1 ± 2.9
80	39.164	Lauric acid	143–07-7	ND	ND	87.1 ± 8.9	ND	ND
81	40.075	Diisobutyl phthalate	84–69-5	38.2 ± 7.4	61.7 ± 4.1	223 ± 35	ND	ND
82	40.093	Phthalic acid, cyclohexyl isohexyl ester	1,000,315–34-0	35.1 ± 7.2	ND	ND	ND	ND
83	42.390	myristic acid	544–63-8	ND	ND	78.0 ± 24.4	ND	ND
84	42.485	Phthalic acid, 6-ethyl-3-octyl butyl ester	1,000,315–17-4	ND	32.3 ± 1.9	ND	ND	ND

(*continued on next page*)

Table 2 (*continued*)

Number	Retention time (min)	Compound name	CAS ID	YMP	DMP	CMP	GMP	BMP
85	45.404	palmitic acid	57–10-3	ND	ND	53.8 ± 5.7	ND	30.6 ± 10.0
86	45.955	1H-Pyrazole, 3-ethyl-4,5-dihydro-	5920-29-6	ND	ND	13.8 ± 2.1	ND	ND

Note: The results were presented as mean ± standard deviation. "ND" indicates not detected.

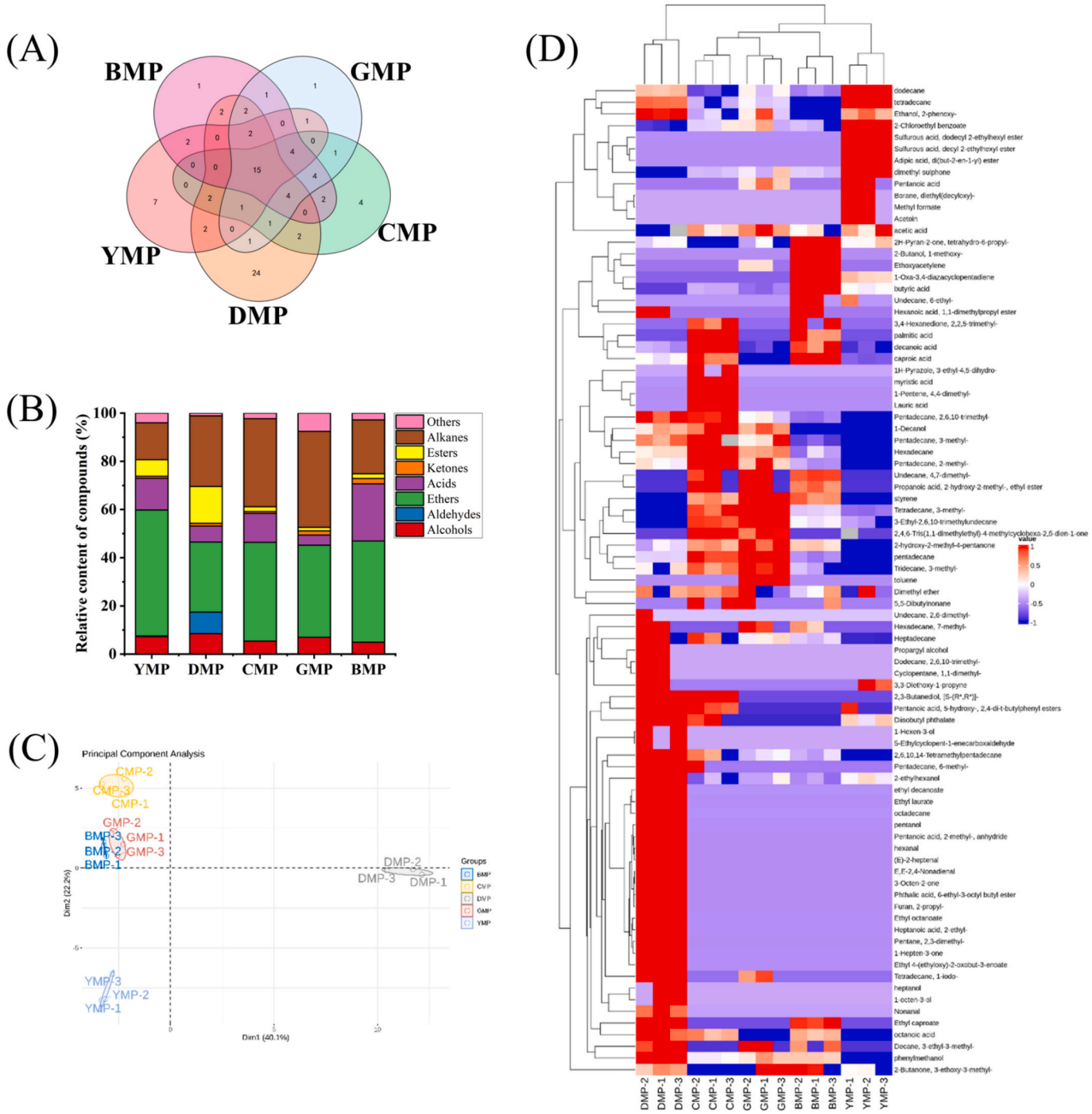

Fig. 6. HS-SPME-GC–MS analysis results of volatile compounds in the five milk powder samples. (A) Venn diagram of volatile compounds. (B) Stacked bar chart of the relative quantities of each type of volatile compound in the five milk powder samples. (C) PCA plot of each type of volatile compound in the five milk powder samples. (D) Hierarchical cluster heatmap of volatile compounds identified by HS-SPME-GC–MS.

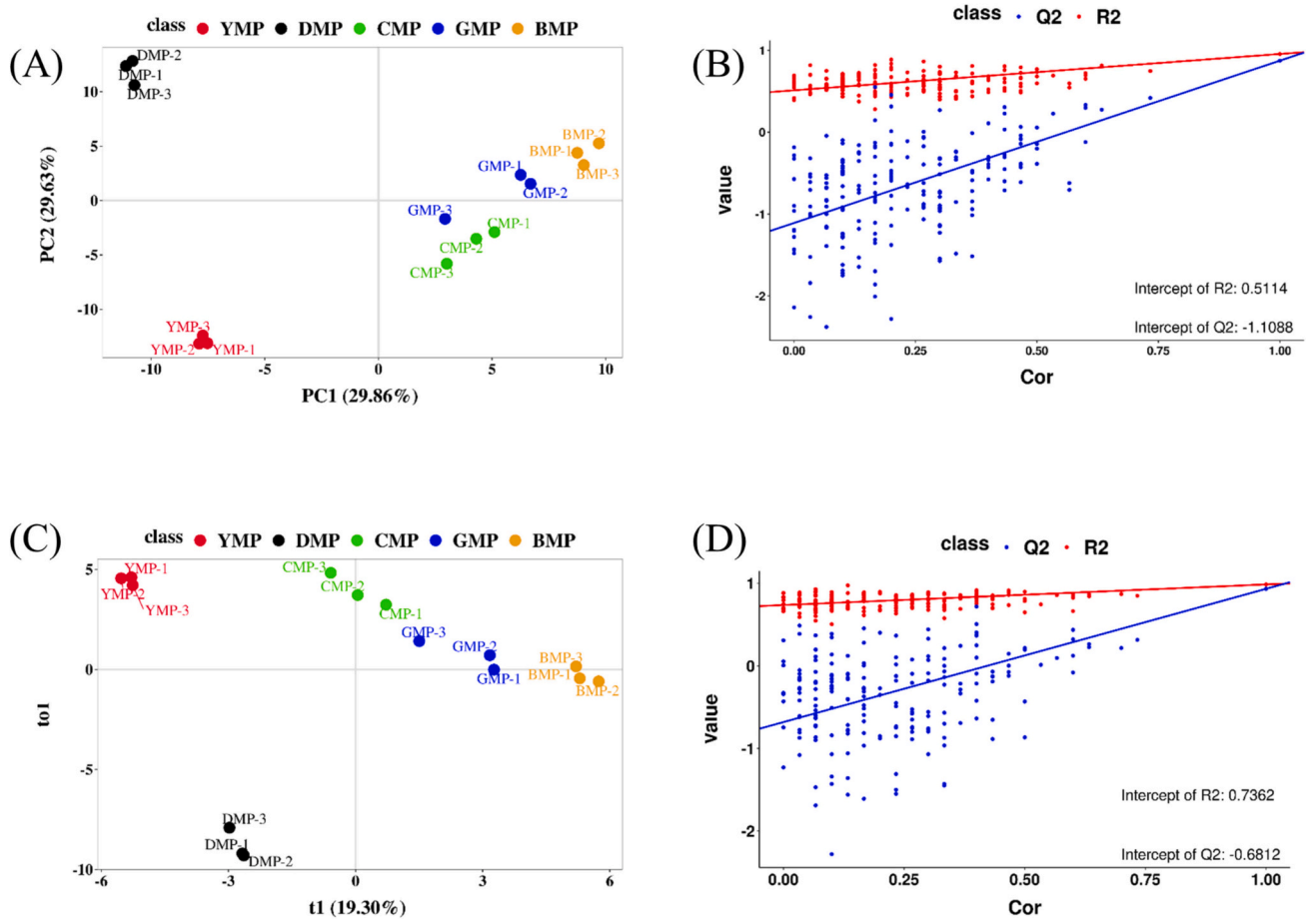

Fig. 7. OPLS-DA and PLS-DA results of volatile compounds identified by HS-SPME-GC–MS. (A) OPLS-DA score plot. (B) OPLS-DA model validation plot (after 200 permutation tests). (C) PLS-DA score plot. (D) PLS-DA model validation plot (after 200 permutation tests).

In addition, we quantified the influence of different volatile compounds on the OPLS-DA model using VIP scores, based on the HS-SPME-GC–MS data. A higher VIP value indicated a greater contribution of a compound to differentiating between milk powder types (Zhang, Lu, et al., 2024). The VIP score plot is shown in Fig. 8A, with detailed VIP values for each volatile compound listed in Table S3. From Fig. 8A, it is evident that 24 volatile compounds, out of the 86 identified by HS-SPME-GC–MS, were characteristic of the milk powders and capable of distinguishing between them (VIP $> 1, p < 0.05$). To further explore the distribution of these compounds, a hierarchical clustering heatmap analysis was performed on the 24 key volatile compounds (Fig. 8B). The analysis revealed distinct differences in the characteristic volatile compounds among the milk powder samples, highlighting their significant role in distinguishing the unique aromas of the various milk powders.

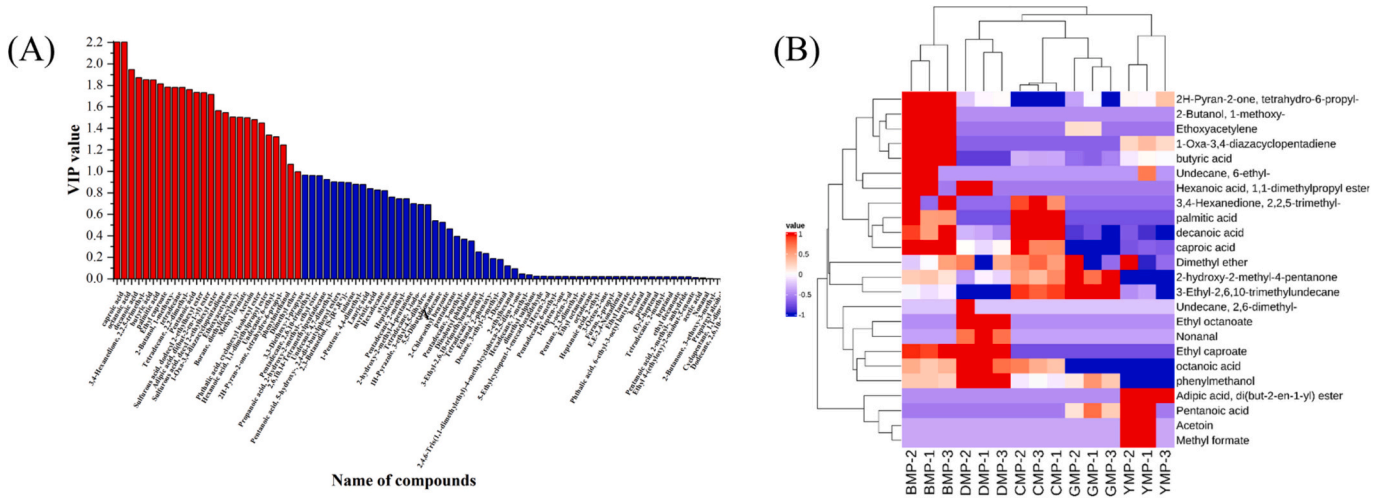

Fig. 8. Screening of key volatile compounds identified by HS-SPME-GC–MS. (A) VIP score plot (based on OPLS-DA results). (B) Hierarchical clustering heatmap analysis of key volatile compounds.

3.7. Combined analysis of HS-GC-IMS and HS-SPME-GC–MS

The data presented above clearly illustrate the complementary advantages of combining the HS-GC-IMS and HS-SPME-GC–MS techniques for a more comprehensive detection of volatile compounds in various milk powder samples. As shown in Fig. S2, there were significant differences in the volatile compound profiles identified by the two methods. Notably, only three compounds were detected by both techniques, underscoring the distinct capabilities of each approach (Chen et al., 2024). This comparison underscores the complementary nature of the two techniques in the analysis of volatile compounds. By combining HS-GC-IMS's rapid, real-time detection with HS-SPME-GC–MS's broad-spectrum detection capabilities, we were able to achieve a more thorough and nuanced understanding of the volatile compounds present in the different milk powders. This integrated approach not only enhances the sensitivity and accuracy of the analysis but also provides deeper insights into the complex aromatic profiles of the milk powders, making it a powerful tool for flavor and aroma research in food science.

Furthermore, Solid Phase Microextraction (SPME) has the ability to capture a broader spectrum of volatile compounds, including those with higher boiling points. This capability is likely one of the key reasons why HS-SPME-GC–MS detected a higher number of phenolic compounds compared to HS-GC-IMS. SPME is particularly efficient in extracting these high-boiling-point volatiles, which are often challenging to capture using other methods (Wang et al., 2020). In contrast, the Ion Mobility Spectrometry (IMS) technique employed in HS-GC-IMS is influenced by ionization processes within the ionization chamber. These processes are shaped by competitive interactions between ion-molecule and ion-ion collisions, which can affect both the sensitivity and selectivity of the detection. As a result, IMS may have reduced sensitivity for certain volatile compounds, particularly those with low volatility or weak ionization responses. This could explain why HS-GC-IMS might identify fewer volatile compounds, especially in complex matrices, compared to more comprehensive techniques like HS-SPME-GC–MS (He, Wu, & Yu, 2021).

In conclusion, each analytical method employed in this study has distinct advantages that contribute to its overall effectiveness. HS-GC-IMS is highly advantageous for rapid, real-time analysis of samples without the need for extensive pre-treatment, making it an ideal choice for quick screenings (Li et al., 2024). On the other hand, HS-SPME-GC–MS provides superior quantitative capabilities and is better suited for identifying a broader range of volatile compounds, especially in complex food matrices. By combining both techniques, we were able to obtain a more nuanced and comprehensive analysis of the volatile profiles in the five milk powder samples, allowing for a more thorough differentiation of their aromatic characteristics. This dual-method approach thus enhanced the overall quality of the volatile compound analysis, providing deeper insights into the flavor profiles of the samples.

4. Conclusions

This study systematically analysed the volatile compounds in five commonly available milk powder samples using both HS-GC-IMS and HS-SPME-GC–MS techniques. A total of 55 volatile compounds were identified by HS-GC-IMS, while 86 volatile compounds were detected using HS-SPME-GC–MS. Multivariate statistical analysis revealed significant differences in the types and concentrations of volatile compounds across the five milk powder samples, allowing for effective differentiation between different types of milk powders. Furthermore, 27 key volatile compounds were identified by HS-GC-IMS, and 24 by HS-SPME-GC–MS, with these key compounds playing a crucial role in distinguishing between different milk powder types. The study highlights the importance of integrating multiple analytical methods to obtain comprehensive information about the volatile compounds in milk powders, which aids in enhancing research on milk powder classification, quality assessment, and sensory characteristics.

This research provides an important theoretical foundation for further exploration of the characteristics and differences in volatile compounds in milk powders, offering valuable insights for the identification and differentiation of various milk powder types. The findings lay a solid foundation for the standardized analysis and quality evaluation of volatile compounds in milk powders, which has significant implications for the development of the dairy industry.

CRediT authorship contribution statement

Yaxi Zhou: Writing – review & editing, Writing – original draft, Supervision, Software, Methodology, Investigation, Formal analysis, Data curation, Conceptualization. **Diandian Wang:** Writing – review & editing, Writing – original draft, Supervision, Software, Methodology, Investigation, Formal analysis, Data curation, Conceptualization. **Jian Zhao:** Visualization, Validation. **Yu Guo:** Visualization, Validation. **Wenjie Yan:** Writing – review & editing, Resources, Project administration, Funding acquisition.

Declaration of competing interest

The authors declare that they have no known competing financial interests or personal relationships that could have appeared to influence the work reported in this paper.

Acknowledgments

This research was supported by the National Key Research and Development Program of China (2023YFF1103802).

Appendix A. Supplementary data

Supplementary data to this article can be found online at https://doi.org/10.1016/j.fochx.2025.102179.

Data availability

Data will be made available on request.

References

Chen, J., Tao, L., Zhang, T., Zhang, J., Wu, T., Luan, D., Ni, L., Wang, X., & Zhong, J. (2021). Effect of four types of thermal processing methods on the aroma profiles of acidity regulator-treated tilapia muscles using E-nose, HS-SPME-GC-MS, and HS-GC-IMS. *LWT, 147*, Article 111585. https://doi.org/10.1016/j.lwt.2021.111585

Chen, J., Wang, W., Jin, J., Li, H., Chen, F., Fei, Y., & Wang, Y. (2024). Characterization of the flavor profile and dynamic changes in Chinese traditional fish sauce (Yu-lu) based on electronic nose, SPME-GC-MS and HS-GC-IM. *Food Research International, 192*, Article 114772. https://doi.org/10.1016/j.foodres.2024.114772

Chen, P., Fu, R., Shi, Y., Liu, C., Yang, C., Su, Y., Lu, T., Zhou, P., He, W., Guo, Q., & Fei, C. (2024). Optimizing BP neural network algorithm for Pericarpium Citri Reticulatae (Chenpi) origin traceability based on computer vision and ultra-fast gas-phase electronic nose data fusion. *Food Chemistry, 442*, Article 138408. https://doi.org/10.1016/j.foodchem.2024.138408

Cheng, L., Wang, Y., Zhang, J., Zhu, J., Liu, P., Xu, L., … Liu, Z. (2021). Dynamic changes of metabolic profile and taste quality during the long-term aging of Qingzhuan tea: The impact of storage age. *Food Chemistry, 359*, Article 129953. https://doi.org/10.1016/j.foodchem.2021.129953

Chi, X., Shao, Y., Pan, M., Yang, Q., Yang, Y., Zhang, X., Ai, N., & Sun, B. (2021). Distinction of volatile flavor profiles in various skim milk products via HS-SPME–GC–MS and E-nose. *European Food Research and Technology, 247*(6), 1539–1551. https://doi.org/10.1007/s00217-021-03730-0

Ditlevsen, K., Sandøe, P., & Lassen, J. (2019). Healthy food is nutritious, but organic food is healthy because it is pure: The negotiation of healthy food choices by Danish consumers of organic food. *Food Quality and Preference, 71*, 46–53. https://doi.org/10.1016/j.foodqual.2018.06.001

Du, H., Chen, Q., Liu, Q., Wang, Y., & Kong, B. (2021). Evaluation of flavor characteristics of bacon smoked with different woodchips by HS-SPME-GC-MS combined with an electronic tongue and electronic nose. *Meat Science, 182*, Article 108626. https://doi.org/10.1016/j.meatsci.2021.108626

Feng, D., Wang, J., Ji, X.-J., Min, W.-X., & Yan, W.-J. (2021). HS-GC-IMS detection of volatile organic compounds in yak milk powder processed by different drying methods. *LWT, 141*, Article 110855. https://doi.org/10.1016/j.lwt.2021.110855

Feng, D., Wang, J., Ji, X.-J., Min, W.-X., & Yan, W.-J. (2021a). Analysis of volatile organic compounds by HS-GC-IMS in powdered yak milk processed under different sterilization conditions. *Journal of Food Quality, 2021*(1), Article 5536645. https://doi.org/10.1155/2021/5536645

Gu, S., Zhang, J., Wang, J., Wang, X., & Du, D. (2021). Recent development of HS-GC-IMS technology in rapid and non-destructive detection of quality and contamination in Agri-food products. *TrAC Trends in Analytical Chemistry, 144*, Article 116435. https://doi.org/10.1016/j.trac.2021.116435

He, J., Wu, X., & Yu, Z. (2021). Microwave pretreatment of camellia (Camellia oleifera Abel.) seeds: Effect on oil flavor. *Food Chemistry, 364*, Article 130388. https://doi.org/10.1016/j.foodchem.2021.130388

Herbert-Pucheta, J. E., Lozada-Ramírez, J. D., Ortega-Regules, A. E., Hernández, L. R., & Anaya de Parrodi, C. (2021). Nuclear magnetic resonance metabolomics with double pulsed-field-gradient echo and automatized solvent suppression spectroscopy for multivariate data matrix applied in novel wine and juice discriminant analysis. *Molecules, 26*(14), 4146. https://doi.org/10.3390/molecules26144146

Hu, M., Wang, S., Liu, Q., Cao, R., & Xue, Y. (2021). Flavor profile of dried shrimp at different processing stages. *LWT, 146*, Article 111403. https://doi.org/10.1016/j.lwt.2021.111403

Jo, Y., Benoist, D. M., Barbano, D. M., & Drake, M. A. (2018). Flavor and flavor chemistry differences among milks processed by high-temperature, short-time pasteurization or ultra-pasteurization. *Journal of Dairy Science, 101*(5), 3812–3828. https://doi.org/10.3168/jds.2017-14071

Junxing, L. I., Aiqing, M., Gangjun, Z., Xiaoxi, L., Haibin, W., Jianning, L., … Chengying, M. (2022). Assessment of the 'taro-like' aroma of pumpkin fruit (Cucurbita moschata D.) via E-nose, GC–MS and GC-O analysis. *Food Chemistry, X, 15*, Article 100435. https://doi.org/10.1016/j.fochx.2022.100435

Lantsuzskaya, E. V., Krisilov, A. V., & Levina, A. M. (2015). Structure of the cluster ions of ketones in the gas phase according to ion mobility spectrometry and ab initio calculations. *Russian Journal of Physical Chemistry A, 89*(10), 1838–1842. https://doi.org/10.1134/S0036024415100179

Li, H., Yang, X., Tang, D., Xi, B., Li, W., Chen, Z., Bao, Y., Dingkao, R., Gao, Y., Wang, P., & Wang, H. (2024). Exploring the link between microbial community structure and flavour compounds of traditional fermented yak milk in Gannan region. *Food Chemistry, 435*, Article 137553. https://doi.org/10.1016/j.foodchem.2023.137553

Li, M., Yang, R., Zhang, H., Wang, S., Chen, D., & Lin, S. (2019). Development of a flavor fingerprint by HS-GC–IMS with PCA for volatile compounds of Tricholoma matsutake singer. *Food Chemistry, 290*, 32–39. https://doi.org/10.1016/j.foodchem.2019.03.124

Li, Q., Zhang, C., Liu, W., Li, B., Chen, S., Wang, H., Li, Y., & Li, J. (2024). Characterization and exploration of dynamic variation of volatile compounds in vine tea during processing by GC-IMS and HS-SPME/GC–MS combined with machine learning algorithm. *Food Chemistry, 460*, Article 140580. https://doi.org/10.1016/j.foodchem.2024.140580

Li, W., Wang, Z., Sun, W., & Bahrami, S. (2023). An ensemble clustering framework based on hierarchical clustering ensemble selection and clusters clustering. *Cybernetics and Systems, 54*(5), 741–766. https://doi.org/10.1080/01969722.2022.2073704

Munblit, D., Crawley, H., Hyde, R., & Boyle, R. J. (2020). Health and nutrition claims for infant formula are poorly substantiated and potentially harmful. *BMJ, 369*, Article m875. https://doi.org/10.1136/bmj.m875

Pan, M., Tong, L., Chi, X., Ai, N., Cao, Y., & Sun, B. (2019). Comparison of sensory and electronic tongue analysis combined with HS-SPME-GC-MS in the evaluation of skim milk processed with different preheating treatments. *Molecules, 24*(9), 1650. https://doi.org/10.3390/molecules24091650

Ping, C., Deng, X., Guo, Z., Luo, W., Li, X., & Xin, S. (2024). Characterizing the flavor profiles of Linjiangsi broad bean (Vicia faba L.) paste using bionic sensory and multivariate statistics analyses based on ripening time and fermentation environment. *Food Chemistry: X, 23*, Article 101677. https://doi.org/10.1016/j.fochx.2024.101677

Qi, H., Ding, S., Pan, Z., Li, X., & Fu, F. (2020). Characteristic volatile fingerprints and odor activity values in different Citrus-tea by HS-GC-IMS and HS-SPME-GC-MS. *Molecules, 25*(24), 6027. https://doi.org/10.3390/molecules25246027

Sager, M., McCulloch, C. R., & Schoder, D. (2018). Heavy metal content and element analysis of infant formula and milk powder samples purchased on the Tanzanian market: International branded versus black market products. *Food Chemistry, 255*, 365–371. https://doi.org/10.1016/j.foodchem.2018.02.058

Shi, S., Feng, J., Yang, L., Xing, J., Pan, G., Tang, J., Wang, J., Liu, J., Cao, C., & Jiang, Y. (2023). Combination of NIR spectroscopy and algorithms for rapid differentiation between one-year and two-year stored rice. *Spectrochimica Acta Part A: Molecular and Biomolecular Spectroscopy, 291*, Article 122343. https://doi.org/10.1016/j.saa.2023.122343

Song, H., & Liu, J. (2018). GC-O-MS technique and its applications in food flavor analysis. *Food Research International, 114*, 187–198. https://doi.org/10.1016/j.foodres.2018.07.037

Sun, P., Lin, S., Li, X., & Li, D. (2024). Different stages of flavor variations among canned Antarctic krill (Euphausia superba): Based on GC-IMS and PLS-DA. *Food Chemistry, 459*, Article 140465. https://doi.org/10.1016/j.foodchem.2024.140465

Wang, S., Chen, H., & Sun, B. (2020). Recent progress in food flavor analysis using gas chromatography–ion mobility spectrometry (GC–IMS). *Food Chemistry, 315*, Article 126158. https://doi.org/10.1016/j.foodchem.2019.126158

Xi, Y., Yang, Y., Chi, X., Wang, W., Sun, B., & Ai, N. (2024). Characterization of the flavor profile of UHT milk during shelf-life via volatile metabolomics fingerprinting combined with chemometrics. *Food Research International, 191*, Article 114705. https://doi.org/10.1016/j.foodres.2024.114705

Yacine Ware, L., Durand, N., Nikiema, P. A., Alter, P., Fontana, A., Montet, D., & Barro, N. (2017). Occurrence of mycotoxins in commercial infant formulas locally produced in ouagadougou (burkina faso). *Food Control, 73*, 518–523. https://doi.org/10.1016/j.foodcont.2016.08.047

Yang, G., Zhang, J., Dai, R., Ma, X., Huang, C., Ren, W., … Liang, C. (2023). Comparative study on nutritional characteristics and volatile flavor substances of yak milk in different regions of Gannan. *Foods, 12*(11), 2127. https://doi.org/10.3390/foods12112172

Ye, Y., Wang, L., Zhan, P., Tian, H., & Liu, J. (2022). Characterization of the aroma compounds of millet huangjiu at different fermentation stages. *Food Chemistry, 366*, Article 130691. https://doi.org/10.1016/j.foodchem.2021.130691

Yormirzoev, M., Li, T., & Teuber, R. (2021). Consumers' willingness to pay for organic versus all-natural milk – does certification make a difference? *International Journal of Consumer Studies, 45*(5), 1020–1029. https://doi.org/10.1111/ijcs.12622

Zhang, F., Lu, B., He, X., & Yu, F. (2024). Flavor variations in precious Tricholoma matsutake under different drying processes as detected with HS-SPME-GC-MS. *Foods, 13*(13), 2123. https://doi.org/10.3390/foods13132123

Zhang, J., Zhong, L., Wang, P., Song, J., Shi, C., Li, Y., … Wen, P. (2024). HS-SPME-GC-MS combined with orthogonal partial least squares identification to analyze the effect of LPL on yak milk's flavor under different storage temperatures and times. *Foods, 13*(2), 342. https://doi.org/10.3390/foods13020342

Zhang, Q., Wang, Y., Meng, F., Wang, B., & Wang, Y. (2024). Comparative analysis of the volatile flavor compounds of Monascus-fermented cheese with different ripening periods by SPME-GC-MS, SPME-GC×GC-MS, and HS-GC-IMS. *Food Bioscience, 62*, Article 105045. https://doi.org/10.1016/j.fbio.2024.105045

Zhao, X., Guo, Y., Zhang, Y., Pang, X., Wang, Y., Lv, J., & Zhang, S. (2023). Effects of different heat treatments on maillard reaction products and volatile substances of camel milk. *Frontiers in Nutrition, 10*, 1072261. https://doi.org/10.3389/fnut.2023.1072261

Zhou, Y., Wang, D., Duan, H., Zhou, S., Guo, J., & Yan, W. (2023). Detection and analysis of volatile flavor compounds in different varieties and origins of goji berries using HS-GC-IMS. *LWT, 187*, Article 115322. https://doi.org/10.1016/j.lwt.2023.115322